

Exploring characteristics of bioelectricity generation and dye decolorization of mixed and pure bacterial cultures from wine-bearing wastewater treatment

Jing-Long Han · Ying Liu · Chang-Tang Chang ·
Bor-Yann Chen · Wen-Ming Chen ·
Hui-Zhong Xu

Received: 14 January 2010 / Accepted: 3 August 2010 / Published online: 22 September 2010
© Springer Science+Business Media B.V. 2010

Abstract This study uncovered microbial characteristics of bioelectricity generation and dye decolorization in single-chamber microbial fuel cells (MFCs) using activated sludge for wine-containing wastewater treatment. Phylogenetic tree analysis on 16S rRNA gene fragments indicated that the predominant strains on anodic biofilm in acclimatized MFCs were Gamma-Proteobacteria *Aeromonas punctata* NIU-P9, *Pseudomonas plecoglossicida* NIU-Y3, *Pseudomonas koreensis* NIU-X8, *Acinetobacter junii* NIU-Y8, *Stenotrophomonas maltophilia* NIU-X2. Our findings showed that the current production capabilities of

these pure strains were only ca. 10% of those of their mother activated sludge, indicating that synergistic interactions among microbes might be the most influential factor to maximize power generation in MFCs. Plus, these electrochemically active strains also performed reductive decolorization of C.I. reactive blue 160, suggesting that bioelectricity generation might be directly associated to azo dye decolorization to deal with electron transfer on anodic biofilm in MFCs.

Keywords Azo dye decolorization · Bioelectricity generation · Microbial fuel cell · Gamma-Proteobacteria

J.-L. Han · Y. Liu · H.-Z. Xu
School of Environmental and Materials Engineering,
Yan-Tai University, Yan-Tai 264005, China

C.-T. Chang (✉)
Department of Environmental Engineering, National
I-Lan University, I-Lan 26047, Taiwan
e-mail: ctchang@niu.edu.tw

B.-Y. Chen (✉)
Department of Chemical and Materials Engineering,
National I-Lan University, I-Lan 26047, Taiwan
e-mail: bychen@niu.edu.tw

W.-M. Chen
Department of Seafood Science, National Kaohsiung
Marine University, No. 142, Hai-Chuan Road, Nan-Tzu,
Kaohsiung City 81157, Taiwan

C.-T. Chang · B.-Y. Chen
Center of Green Technology (G-TEC), National I-Lan
University, I-Lan, 26047, Taiwan

Introduction

To simultaneously resolve the worldwide problems of gradually worsened environmental pollution and energy crisis, recently much attention on bioelectricity generation via microbial fuel cells (MFCs) for wastewater treatment has been paid for renewable energy generation (Rabaey and Keller 2008). In fact, wastewater treatment via MFC mainly focused on removal of COD, carbon or nitrogen source (Virdis et al. 2008), treatment of sulfite and thiosulfate. Plus, MFCs could also be applied to several practical situations; for example, using MFCs as BOD sensors (Moon et al. 2004) and in situ measurement for

bioremediation could show a promising operation stability of at least over 5 years with minimum maintenance (Chang et al. 2004). Moreover, recently advanced technology for on-site measurement (Logan et al. 2006) and state of the art information and significant progress on MFCs (Du et al. 2007) made MFC more technically feasible for practical uses.

As a matter of fact, numerous factors could significantly affect MFC performance; namely, the types of microbial inoculums (Cheng and Logan 2007), fuel cell configuration (Fan et al. 2007; Fornero et al. 2008), electrode materials (Moon et al. 2006; Zhao et al. 2005) and operating conditions (e.g., pH buffer, organic loading rate, the concentration of electron acceptors, and types of carbon and nitrogen substrates) (Gil et al. 2003; Park and Zeikus 2003; Pham et al. 2004; Pant et al. 2010). In materials science, several new electrode materials (e.g., Pt-carrying electrode, metal mesh cathode; Pant et al. 2010) have been recently developed to significantly augment power density (ca. >1220 mW/m²) in MFCs. However, exploring the most promising electrochemically active microbe(s) as electron transfer mediator(s) still played a crucial role in articulating MFC as a “subversive subject” of renewable bioenergy for sustainable development. Thus, we have mainly focused this research on microbial characteristics of electrochemically active microorganisms in MFCs from indigenous bioresource for sustainable uses, since only bacterial cultures with high-level electrochemical capability were the most feasible for long-term stable bioelectricity generation of MFC operations.

Although various MFCs using mixed consortia were regularly mentioned in literature, detailed characteristics of bioelectricity generation using pure strains are seldom elucidated. Thus, whether bioelectricity-generation characteristics of pure strains or combined interactions among species (e.g., synergistic relationships) to deal with high efficiencies of electron transfer was still remained unsolved to be disclosed for system optimization. Eventually, lack of these adequate evolutionary figures at microbiological levels makes the performance of MFCs unpredictable and unreliable for long-term practical uses. Up to now, at least 20 pure bioelectricity-generating bacteria have been reported in literature (Zhang et al. 2010). Erable et al. (2010) also revealed that current density generated by mixed cultures was better than

that produced by pure strains, likely due to synergistic (or cooperative) interactions among microbes on the anode to significantly enhance current production. However, there were still few comparative analyses on MFCs of pure and mixed cultures under specific conditions to verify this proposed concept (Logan 2008). Here, this first-attempt study tended to uncover these unsolved mysteries via quantitative assessment upon power generation of pure and mixed culture MFCs.

Since at least over 10,000 kinds of textile dyes and pigments were used in textile dyeing and printing industries worldwide, dye-bearing wastewater apparently was one of the top-priority pollutants to be treated due to its visible color and potential biotoxicity to natural lives. Among all dyes, azo dyes were the most frequently used (>60%) for industrial textile dyeing since they were in particularly designed to be in low biodegradability ($BOD_5/COD < 0.2$; Asad et al. 2007). Regarding dye removal, compared to biotreatment, using other alternative means (e.g., physical and chemical methods such as adsorption, membrane treatment and photodegradation) (Gogate and Pandit 2004; Shu et al. 2004) was not economically feasible and environmentally-friendly due to the potential impact to introduce secondary pollution to natural environment (Maier et al. 2004). According to the mechanism of azo dye biodegradation, capabilities of reductive biodecolorization of azo dyes are also strongly associated to characteristics of electron transfer via electron-transport chain (e.g., reduced coenzyme NADH, ubiquinone (Q) and cytochrome C as electron shuttles and donor) (Chen 2002; Hsueh et al. 2009; Zhang et al. 2010). That is, whether this electron-releasing capability of bacterial decolorizer is related to cellular electron-transport chain for bioelectricity generation is still remained open to be discussed. Recently, Sun et al. (2009b) and Chen et al. (2010a, b) reported the promising feasibility of dye decolorization accompanied with bioelectricity generation using mixed and pure culture single-chamber MFC systems, respectively. Cao et al. (2010) used glucose, acetate sodium and ethanol as energy substrates for simultaneous decolorization and bioelectricity generation. Their findings indicated that >98% of Congo red could be decolorized in 36 h using a proton exchange membrane (PEM) air-cathode single-chamber MFC. In addition, Li et al. (2010) found that MFCs operated at higher power

densities could simultaneously increase COD removal efficiency as well as the rate of dye decolorization, even though bioelectricity generation seemed to be competitive to dye decolorization. Due to aforementioned points, Chen et al. (2010a) thus proposed that some decolorized intermediate(s) might play a role to enhance rate of oxidative phosphorylation as well as electron transport for power generation.

Here, this study first explored the characteristics of bioelectricity generation of pure and mixed microbial cultures using glucose, sodium acetate at different concentrations as substrates for comparison. Next, we specifically isolated predominant strains from the anodic biofilm in single chamber membrane less MFCs for species identification. Phylogenetic tree analysis of 16S rRNA revealed that these predominant strains were all belong to Gamma Proteobacteria (e.g., *Aeromonas punctata*, *Pseudomonas plecoglossicida*, *P. koreensis* obtained from glucose acclimation and *Acinetobacter junii*, *Stenotrophomonas maltophilia* selected from sodium acetate acclimation). Here, this study also used predominant strains of activated sludge obtained from wine-bearing treatment plant as inoculating sources of MFCs for treatability assessment on dye-treatment. This feasibility study of dye decolorization using these predominant strains in MFCs also revealed that using wine-containing wastewater as cometabolic substrates for simultaneous bioelectricity generation and dye treatment should be technically viable. This would significantly reduce operation cost for industrial dye decolorization, since augmentation of secondary carbon source of cometabolism to simulate reductive decolorization is inevitable.

In this model study, we intentionally explored the performance of current production and dye decolorization of mixed consortia and isolated strains obtained from the activated sludge for wine-bearing wastewater treatment plant in Yilan Distillery, north-east Taiwan. To the best of our knowledge, this is a first attempt to decipher microbial characteristics of bioelectricity generation of both predominant strains (e.g., *Ae. punctata*, *P. plecoglossicida*, *P. koreensis*, *Ac. junii*, *S. maltophilia*) and their mother mixed consortia in MFCs, indicating that synergistic interactions of bioelectricity generation among microbes are of great importance to maximize power generation in MFC systems.

Materials and methods

MFC construction

The single chamber air-cathode mediator-less, membrane-less MFCs (ML-MFCs) were constructed in cylindrical tanks made by polymethyl methacrylate (PMMA) (OD = 59 mm, ID = 55 mm and electrode spacing L = 90 mm) with working volume of ca. 200 ml. The anode electrode was originally constructed from activated carbon cloth (without catalyst) (CeTech™, Taiwan) while a hydrophobic carbon cloth (purchased from CeTech™, Taiwan) was used as the matrix of the cathode (a projected area of ca. 23 cm²). The air cathode was almost identical to the anode in size and consisted of a polytetrafluoroethylene (PTFE) diffusion layer (CeTech™, Taiwan) on the air-facing side. Electrodes were connected externally with concealed copper wire through external load resistance. Prior to construction of MFC, 3.0% H₂O₂ was completely filled in chambers for 1 day to guarantee complete sterilization (Chen et al. 2009a, b, c). Then, H₂O₂ was washed out by sterile deionized-and-distilled water for 1 day clean-up prior to the study. The sterile conditions were also confirmed via traditional plate-count techniques.

Cell culture and growth media

The activated sludge (ca. 100 ml 1.0 g VSS/l) taken from the wine-bearing wastewater treatment plant of Yilan Distillery, TTL Corp. (Taiwan Tobacco & Liquor Corporation) was inoculated for mixed consortium-bearing single chamber ML-MFCs. As known, wine-bearing wastewater contained high-level COD and natural pigments (Bharagava and Chandra 2010; Mohanakrishna et al. 2010). That was why we intentionally chose activated sludge obtained from wine-bearing wastewater treatment plant as microbial seeding for this MFC study. For acclimation of this sludge using different carbon sources, seed cultures taken from activated sludge were precultured in minimum minerals (MM) medium containing 500 mg COD/L sodium acetate or glucose for 2 months. Plus, a half of the culture broth was replaced with sterile fresh medium every 48 h to guarantee maximal metabolic cellular activity to be stably maintained. The MM medium contained Na₂CO₃ 0.5 g/l, MgSO₄•7H₂O 0.15 g/l, KH₂PO₄

1.0 g/l, K₂HPO₄ 1.0 g/l, ZnSO₄•7H₂O 2.2 mg/l, CaCl₂•2H₂O 7.3 mg/l, MnCl₂•4H₂O 2.5 mg/l, CoCl₂•6H₂O 0.5 mg/l, FeSO₄•7H₂O 5.0 mg/l and CuSO₄•5H₂O 0.2 mg/l. Cultured cells were then added into ML-MFCs for cell propagation and anodic biofilm formation after two-month preculture. For acclimatization in MFCs, half of the medium in the MFC chamber was replaced by fresh medium, when cell voltage dropped to ca. 1/10 of the maximal output voltage. The MFC system was considered to be under steady-state operation when its maximal output voltage was stably reproduced after at least three cycles of medium replacement. Once the stability and reproducibility of current production were confirmed, batch-fed MFC experiments at various conditions for current production were carried out. For pure culture-containing MFCs, the pure predominant isolates were selected from microbial communities in anodic biofilms of glucose- or acetate-acclimatized MFCs. To guarantee the purity of isolates for strain identification, five cycles of serial streak isolation for predominant strains were carried out as described elsewhere (Chen et al. 2009a). Then, the procedures of cell immobilization onto anodic biofilm and batch-fed MFC experiments of pure cultures were followed as mentioned previously for mixed culture MFCs.

Analytical methods and calculations

Power generation

Cell voltage was automatically measured (set at one data point per minute) through a data acquisition system (DAS 5020; Jiehan Technology Corporation) for external resistance R_{out} = 1000 Ω. Note that a relatively high resistance (1000 ohms) was intentionally used herein for comparison of this study with prior studies (Zhang et al. 2010) and literature data (Chen et al. 2010a, b). The polarization curve was obtained through the change of external resistance within electrochemical workstation (ECW-5000, Jiehan Technology Corporation). The power density (P) for an MFC in fed-batch mode can be calculated as follows:

$$P = \frac{U \cdot I}{\text{Area}} \quad (1)$$

where U is the voltage between anode and cathode (V), I is the current (A), Area denoted the anode area

(ca. 0.0023 m²); COD removal efficiency (η_{COD}) during operation could be estimated as follows:

$$\eta_{COD}(\%) = \left(1 - \frac{COD_{out}}{COD_{in}} \right) \times 100\% \quad (2)$$

where COD_{in} and COD_{out} represented the initial and outlet concentration (mg/l), respectively. According to the fractional conversion of COD removal, the coulombic efficiency (CE) could be calculated as shown in Eq. 3:

$$CE(\%) = \frac{M \int_0^t Idt}{F \cdot b \cdot V \cdot \Delta COD} \times 100\%, \quad (3)$$

where M represented the molecular weight of substrate; F is Faraday's constant (i.e., 96,485 C); b represented number of electrons exchanged per mole of substrate utilized; V was the working volume of MFC; ΔCOD depicted change in COD over operation period of time. Note that the COD was determined as described in US EPA method 410.3 (http://www.epa.gov/waterscience/methods/method/files/410_3.pdf).

Dye decolorization

A loopful of bacterial seed strains (i.e., *Ae. punctata*, *P. plecoglossicida*, *P. koreensis*, *Ac. junii*, *S. malophilia*) taken from an isolated colony on a LB-streak plate was precultured in 50 ml LB broth (casein peptone 10 g/l, yeast extract 5 g/l, sodium chloride 10 g/l) for 12 h at 30°C, pH 7.0 and 200 rpm. Then, color removal experiments were undertaken as described elsewhere (Chen et al. 2009a, b). Azo dye C.I. reactive blue 160 (RB160; λ_{max} = 616 nm) was selected for comparative assessment upon decolorization of isolated strains. All dye solutions were sterilized by filtration of Acrodisc syringe 0.22 μm filter units, as textile dyes may be heat-sensitive in moist-heat sterilization. With appropriate calibrations at specific wavelengths, concentrations of biomass (λ_{max} = 600 nm) and RB160 were determined using an UV-Visible spectrophotometer (HITACHI Spectrophotometer, model UV-2001). The concentration of dye was primarily determined by measuring the optical density (OD) of the supernatant of the sample after centrifugation for 5 min at 700×g (HSIANGTAI Centrifuge MCD-2000). The concentrations of biomass and dye were evaluated as described elsewhere

(Chen 2002). Since the function of cell density (X) and dye concentration ($[Dye]$) are continuous, strictly monotonic and differentiable for all time, their differential terms dX and $d[Dye]$ could thus be denoted by forward-difference formula (e.g., $dX \cong X|_{t+\Delta t} - X|_t = \Delta X$, $d[Dye] \cong [Dye]|_{t+\Delta t} - [Dye]|_t = \Delta [Dye]$) for specific rate determination (e.g., SGR, SDR). To ensure the step size Δt sufficiently small enough for convergence, numerical differentiations were compared with differentiations by reducing step size as $\Delta t/2$ (i.e., $\|(df|_{\Delta t} - df|_{\Delta t/2})\| / \|df|_{\Delta t}\|$). Only the error term less than 1% was then indicated that the calculated tolerance was achieved convergent criteria. Otherwise, the step size Δt was reduced by half for approximations until convergence was achieved. Therefore, specific growth rate (SGR) μ , and specific decolorization rate (SDR) q_P could be calculated (Chen et al. 2009a, c) as

$$SGR = \mu = d\ln X/dt \cong (1/X)(/\Delta t) \text{ and}$$

$$SDR = q_P = -(1/X)(d[Dye]/dt) \cong -(1/X)(\Delta [Dye]/\Delta t),$$

respectively; where X , $[Dye]$, and t were cell concentration, dye concentration, and time, respectively.

Morphological and biochemical test

Morphological examination was observed by a light microscope (Zeiss Axioskop). Gram Stain Set S (BD, USA) and the Ryu non-staining KOH method (Powers 1995) were used to ascertain the Gram reaction. Biochemical identification presented in the Microgen ID microtests was determined by Microgen ID software Version 1.1.16.19 according to the recommendation of the manufacturer (Microgen Bioproducts, UK).

16S rRNA gene sequencing and phylogenetic analysis

Amplification and sequence analysis of the 16S rRNA gene was performed as described previously (Chen et al. 2001). The sequence was compared with others available in GenBank. The multiple-sequence alignment of closest relatives was performed using the BioEdit program. The phylogenetic reconstruction was inferred by using the neighbor-joining method in the BioEdit software. A bootstrap analysis (confidence

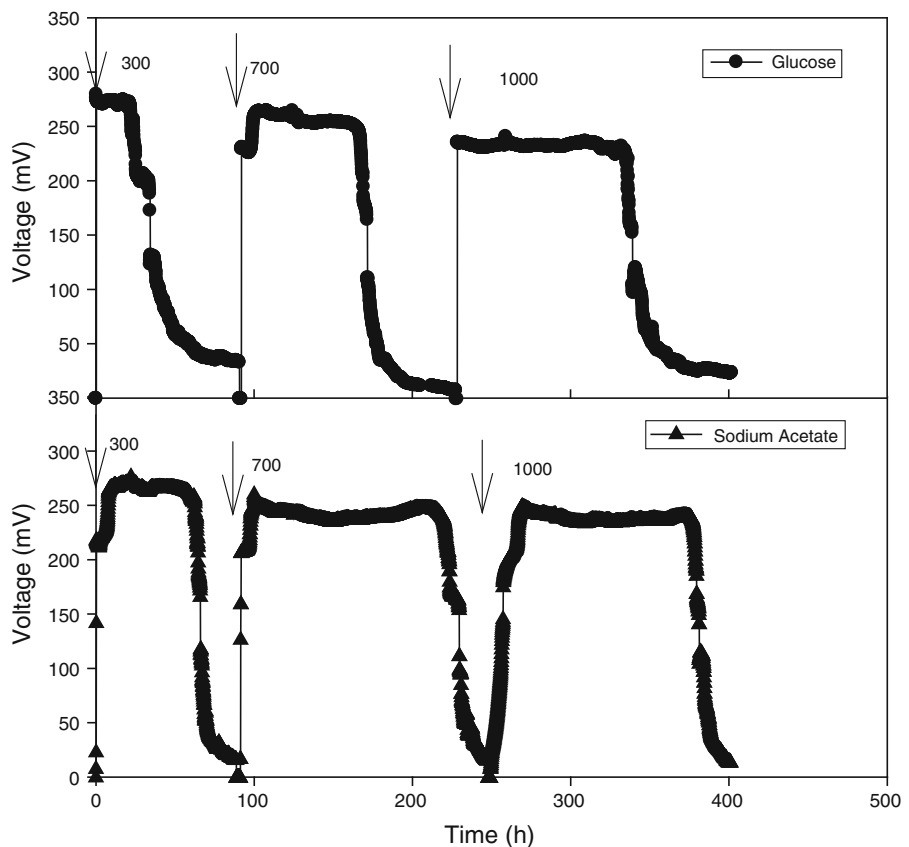
values estimated from 1000 replications of each sequence) was performed for the neighbor-joining analysis using the CLUSTAL w 1.7 program (Thompson et al. 1997). A phylogenetic tree was drawn using the TREEVIEW program (Page 1996). Sequence identities were calculated using the BioEdit program.

Results and discussion

The effect of initial substrate concentration

As shown in Figs. 1, 2 and Tables 1, 2 for mixed culture MFCs, cell voltage was rapidly increased once fresh substrate was supplemented (i.e., insignificant lag for power generation), indicating that more biodegradable substrates sufficiently provided in fresh substrate could be oxidized more effectively for electron transfer via oxidative phosphorylation towards anodic biofilm in MFCs. Plus, average current density and coulombic efficiency slightly decreased as substrate concentration increased (e.g., low (101.3 mA/m^2 , 44.64 mW/m^2) at 1000 mg COD/l and high (118.4 mA/m^2 , 75.99 mW/m^2) at 300 mg COD/l for glucose, and low (102.8 mA/m^2 , 48.91 mW/m^2) at 1000 mg COD/l and high (115.7 mA/m^2 , 81.25 mW/m^2) at 300 mg COD/l for acetate)). In fact, longer period of time to maintain stable power generation was observed at higher initial glucose or acetate concentration (e.g., 180 h for 1000 mg COD/l glucose). This suggested that high COD loadings seemed to express the effect of substrate “inhibition” on conversion to power generation. However, higher substrate concentration could provide more electrons to sustain longer duration of power generation. These all suggest that power generation in MFC is growth associated. Apparently, stably maintaining maximal metabolic activity of cells on anodic biofilm would be extremely significant for optimal MFC operation. Plus, CE values for the COD loading at 300 , 700 , 1000 mg/l during gradual shift-up of glucose and acetate concentration was 8.14 , 4.91 and 4.61% (glucose); and 14.4 , 10.5 and 9.27% (acetate), respectively. This pointed out that higher fraction of electrons were transferred from substrate oxidation as electrical current at lower substrate concentration. In addition, higher COD loadings might entice more substantial competition between fermentative microbes and electrochemically active bacteria, resulting in greater COD

Fig. 1 Comparison of cell voltage output during shift-up of glucose and acetate concentrations for repeated fed-batch cycles in two acclimatized mixed-consortium MFCs (unit: COD mg/l; $R_{out} = 1000 \Omega$)



removal not used for current production (Lorenzo et al. 2010). In contrast, at lower substrate concentrations, it would be more thermodynamically favorable for substrate utilization of bioelectricity-generating bacteria to produce bioelectricity. In addition, as part of COD removal was used for aerobic degradation rather than bioelectricity generation, lower CE values (max. 8.14 and 14.4% for glucose and acetate, respectively) in MFCs were resulted (Sun et al. 2009a, b). Moreover, these lower CE values also indicated that electrons generated from bacterial oxidation of organic substrate were possibly consumed by oxygen as the electron acceptor (Cheng et al. 2006). As shown in profiles of voltage output and related characteristics using glucose and acetate at different COD loadings as substrates (Fig. 1; Tables 1, 2), the maximum average power densities taking place at glucose and acetate of 300 mg/l COD were 75.99 and 81.25 mW/m², respectively. According to Logan (2008), the maximum power took place at the point where the internal resistance equals the external resistance (i.e., internal resistance of 218 ± 12 and $189 \pm 15 \Omega$ for glucose

and acetate, respectively). Due to increased internal resistance to deliver electrons (i.e., increases in ohmic loss), relatively lower power densities for glucose were obtained. Moreover, since current generation is growth-associated, differences in power densities obtained at glucose and acetate were resulted from diverse substrate uptake rate of microbes via different metabolic pathways (e.g., EMP pathway and TCA cycle for glucose and acetate degradation, respectively).

Microbiological Identification and bioelectricity generation characteristics

We also isolated microbes from anodic biofilm to understand which predominant strains played crucial roles in bioelectricity generation in MFCs. First, with the extraction of intracellular protein after cell disruption upon isolates, SDS-PAGE (sodium dodecyl sulphate-polyacrylamide gel electrophoresis) was used to distinguish the difference of isolated strains. The complexity and molecular masses of constituent polypeptide in cell extracts could be clearly revealed

Fig. 2 Polarization curves to reveal different voltage and power density generated from (a) glucose-acclimatized MFC and (b) sodium acetate-acclimatized MFC at concentration of 300, 500, 700 and 1000 COD mg/l expressed as a function of current density

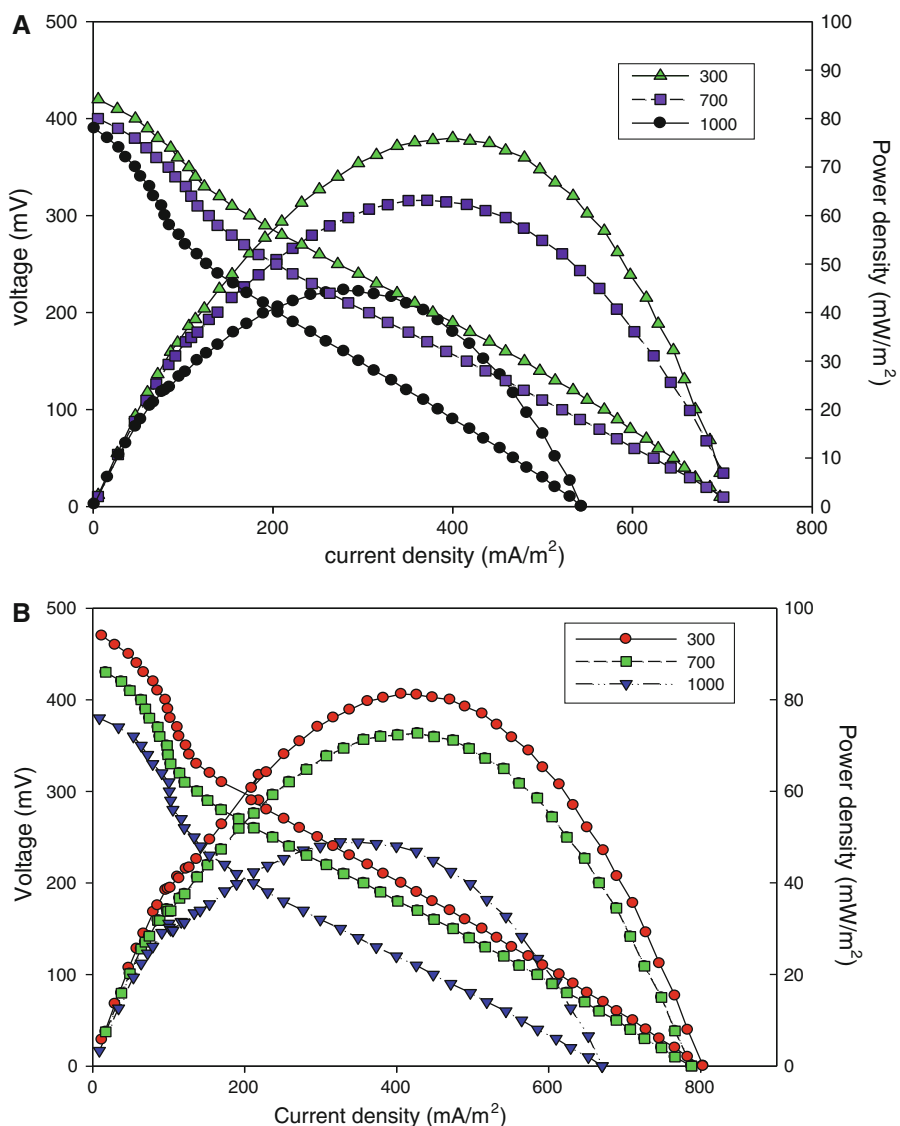


Table 1 List of average current density, average power density, COD removal efficiency and Coulombic efficiency at different initial glucose concentrations

Substrate concentration(COD mg/l)	Average current density (mA/m ²)	Average power density ^a (mW/m ²)	COD removal (%)	Coulombic efficiency (%)
300	118.4	75.99	76.7	8.14
700	110.8	63.14	87.1	4.91
1000	101.3	44.64	92.1	4.61

^a Calculated from values at the plateau of output voltage

in SDS-PAGE. If two prokaryotic isolates are genotypically identical, the profiles of protein expression shown in SDS-PAGE should be identical (i.e.,

phenotypically and/or proteomically identical) under the same operation conditions. Thus, it could be used as a pre-screening technique via a direct match or

Table 2 List of average current density, average power density, COD removal efficiency and Coulombic efficiency at different initial sodium acetate concentrations

Substrate concentration (COD mg/l)	Average current density (mA/m ²)	Average power density ^a (mW/m ²)	COD removal (%)	Coulombic efficiency (%)
300	115.7	81.25	77.3	14.38
700	103.4	72.68	87.2	10.49
1000	102.8	48.91	91.6	9.27

^a Calculated from values at the plateau of output voltage

not-match of individual protein fingerprints. According to SDS-PAGE profiles for protein translation, we found that most of the predominant isolates obtained from acetate- and glucose-acclimatized microbial consortia were similar in protein expression (i.e., proteomically similar; data not shown). Further biochemical identification by Microgen ID microtest system indicates that several isolated strains were also similar to each other. Only three predominant strains isolated from glucose-acclimatized MFCs (NIU-P9, NIU-X8, NIU-Y3) and two from acetate-acclimatized MFCs (NIU-X2, NIU-Y8) were obtained to determine their sequences of 16S rRNA gene. Based on the sequence identity of 16S rRNA gene, the highest similarity values of strain NIU-P9 were obtained towards type strains of *Aeromonas punctata* subsp. *caviae* ATCC 15468^T (99.9% identity) and *Aeromonas punctata* subsp. *punctata* NCIMB 13016^T (99.7% identity). In addition, strain NIU-X8 was in 99.8% nucleotide identity towards type strain *Pseudomonas koreensis* Ps 9-14^T. Strain NIU-X2 was in 99.0% nucleotide identity towards type strain *Stenotrophomonas maltophilia* ATCC 13637^T. Plus, strain NIU-Y8 was in 98.0% nucleotide identity towards the type strain *Acinetobacter parvus* LUH 4616^T. Moreover, strain NIU-Y3 was very similar to type strains *Pseudomonas plecoglossicida* FPC 951^T (99.5%) and *Pseudomonas monteilii* CIP 104883^T (99.5%) (Fig. 3). Apparently, diverse predominant strains would be resulted from different selection pressures (e.g., acetate and glucose) for acclimatization and strain isolation although the predominant strains were all γ -Proteobacteria. That is, using an appropriate nutrient substrate for acclimation and strain isolation upon mixed consortia would trigger a promising evolutionary process for current production. To the best of our knowledge, this is a first systematic report through a random probing of acetate and glucose-acclimatization upon mixed

consortia in MFCs to generalize the presence of predominant strains for bioelectricity generation. Figure 4 indicated that capabilities of bioelectricity generation of five pure strains were only approx 10% of the original mixed consortia (Fig. 1), suggesting that synergistic interactions among microbes in activated sludge might play a crucial role to maximize power generation in MFCs.

Decolorization of isolated cultures

As indicated in Fig. 5, dye decolorization of isolated strains reached a maximal value when cell growth had nearly stopped at the stationary phase, suggesting that color removal was not growth-associated. That is, specific growth rate (SGR) progressively decreased to approximately zero and specific decolorization rate (SDR) gradually increased. However, once SDR reached a maximum value after static incubation, color removal performance gradually decreased. This decrease in decolorization might be due to a significant accumulation of inhibitory intermediates (i.e., aromatic amines), which were formed by a cleavage of azo-bonds. In addition, exhaustion of essential nutrients (e.g., basic growth factors and essential energy sources) and formations of inhibitory products might limit cells to gain energy for bacterial decolorization. According to the maximal SDR (unit in mg l⁻¹ ODU⁻¹ h⁻¹) of RB160, the relative rankings of isolated strains in a decreasing order were *Aeromonas punctata* NIU-P9(6.42) > *Pseudomonas koreensis* NIU-X8(5.82) > *Pseudomonas plecoglossicida*

Fig. 3 Neighbor-joining showing phylogenetic positions of isolated strains and related species based on 16S rRNA gene sequence comparisons. Bootstrap values are indicated at nodes. Only bootstrap values >50% are shown. Scale bar, 1% sequence dissimilarity (one substitution per 100 nt). Representative sequences in the dendrogram were obtained from GenBank (accession number in parentheses)

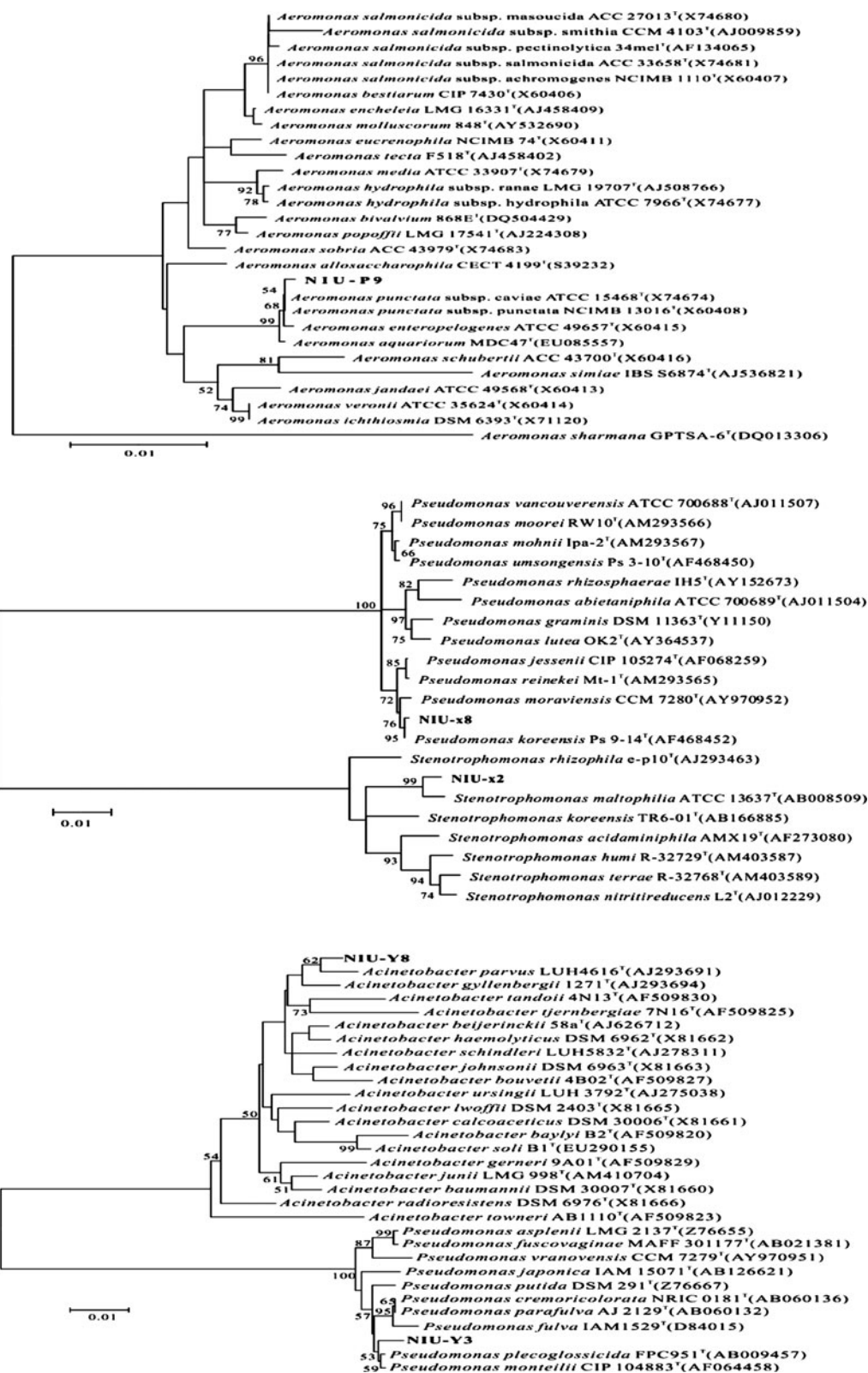


Fig. 4 Comparison of cell voltage output during gradual shift-up of substrate concentration for repeated fed-batch cycles in various pure culture MFCs (arrows denoted added substrate COD mg/l)

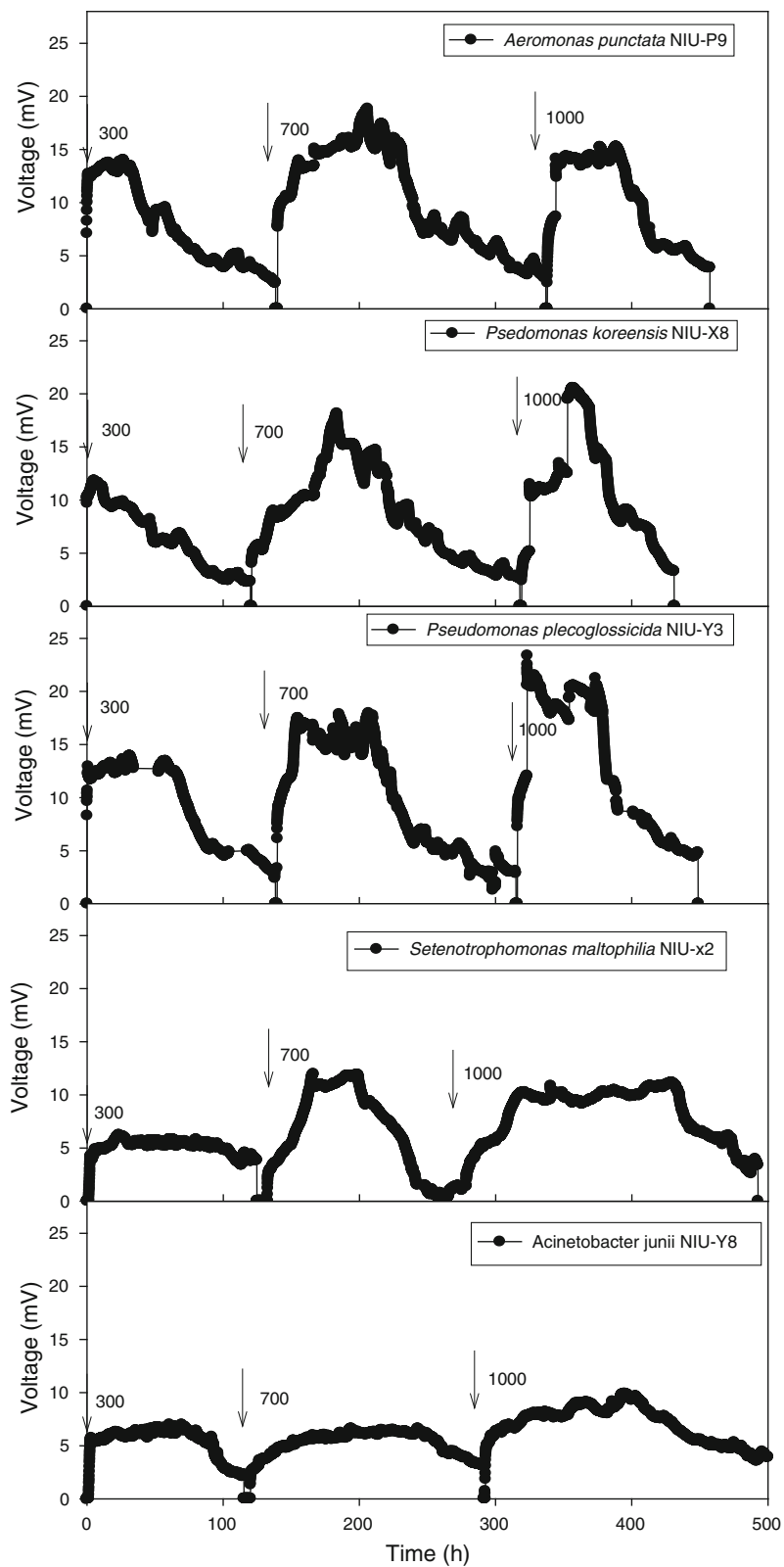
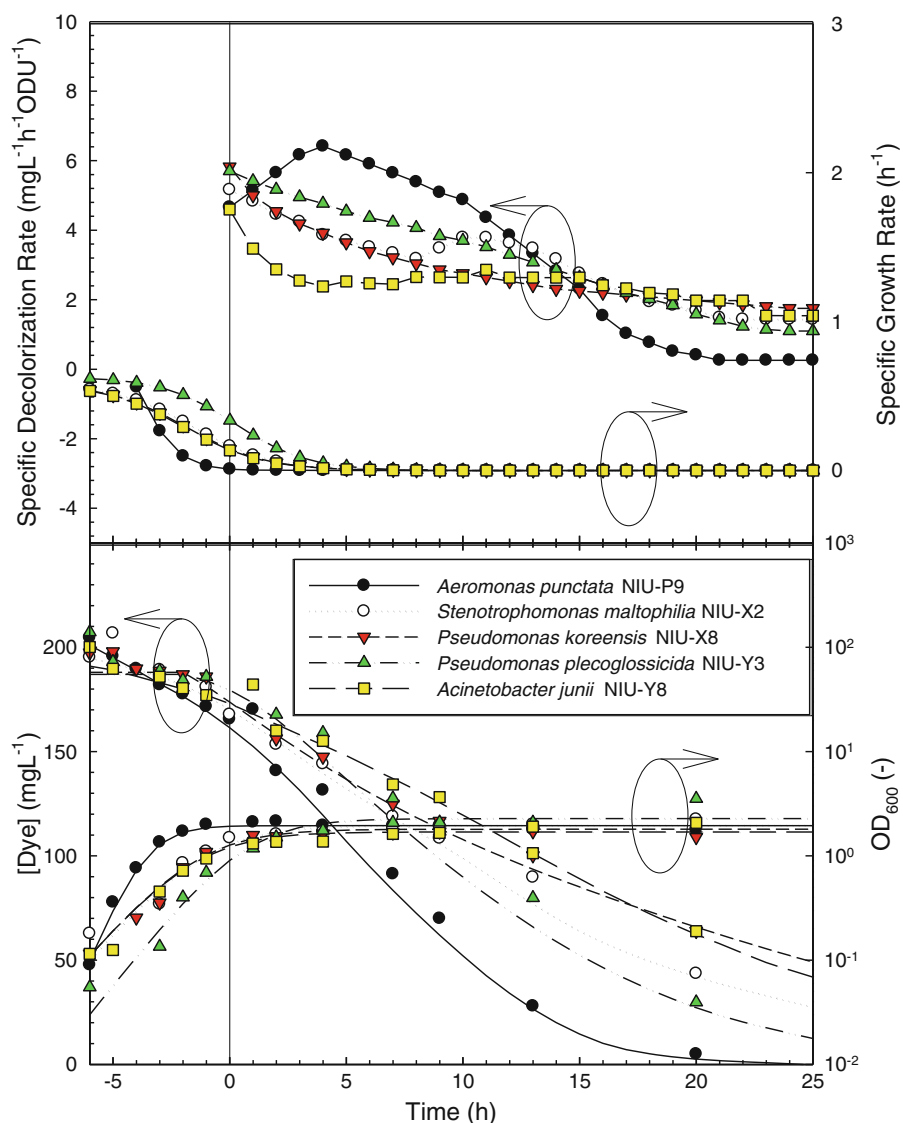


Fig. 5 Time courses of cell growth, color removal, specific decolorization rate and specific growth rate for isolated strains NIU-P9, NIU-X2, NIU-X8, NIU-Y3, NIU-Y8



NIU-Y3(5.70) > *Stenotrophomonas maltophilia* NIU-X2(5.16) > *Acinetobacter junii* NIU-Y8(4.60) (Fig. 5). These SDR values of RB160 were apparently lower than those of *A. hydrophila* NIU01(21.8) > *A. hydrophila* YT11(15.4) > *P. hauseri* ZMd44(14.6) > *A. hydrophila* NIUx73(12.4) > *Ac. johnsonii* NIU x72(7.53) as mentioned in prior findings (Zhang et al. 2010; Hsueh et al. 2009; Shih et al. 2010). Moreover, according to our prior findings on strain isolation, we also suspected that γ -Proteobacteria might be resulted if azo dye decolorization was chosen as the probing characteristics for strain isolation upon myriads of indigenous samples. Plus, the characteristics of azo dye

decolorization might be used as a simple criterion for preliminary screening upon possible candidate electrochemically-active microorganisms from microbial communities of myriads of bioresources for current generation.

Conclusion

At the same COD loadings, the increased internal resistance to deliver electrons (i.e., an increase in ohmic loss) resulted in relatively lower power densities of glucose than acetate. For mixed and pure

cultures of activated sludge for wine-bearing wastewater treatment, microbial characteristics of bioelectricity generation were very possibly associated with the capabilities of reductive decolorization. Predominant electrochemically active microorganisms were found to be γ -Proteobacteria even glucose and acetate-acclimatized mixed consortia were used as different selection pressures. Plus, synergistic interactions among microbes rather than the electrochemical activity of pure predominant strains played a crucial role for effective power production in MFCs.

Acknowledgments This study was completed as part of cooperative achievements for academic exchange program between Yan-Tai University (China) and National I-Lan University (Taiwan) in 2009–2010. The authors sincerely appreciate financial supports (NSC 96-2221-E-197-012, NSC 97-2221-E-197-019, NSC 98-2621-M-006-007 and NSC 98-2221-E-197-007-MY3^{sdg}) from Taiwan's National Science Council for this research. Seeding grants for the project of Microbial Fuel Cell (MFC) of National I-Lan University from Taiwan's Ministry of Education and for the project of "Development of Waste Minimization and Recycling Technology of Petrochemical Industry" (98-EC-17-A-10-S2-0070) from Taiwan's Ministry of Economic Affairs for this work are very much appreciated. The authors gratefully acknowledge Distinguished Professor Jo-Shu Chang (Department of Chemical Engineering, National Cheng-Kung University, Tainan, Taiwan) and Professor Tai-Lee Hu (Department of Environmental Engineering and Science, Feng-Chia University, Taichung, Taiwan) for kindly suggesting valuable comments for the work. The authors also sincerely appreciate significant comments from anonymous reviewers.

References

- Asad S, Amoozegar MA, Pourbabae AA, Sarbolouki MN, Dastgheib SMM (2007) Decolorization of textile azo dyes by newly isolated halophilic and halotolerant bacteria. *Bioresour Technol* 98(11):2082–2088
- Bharagava RN, Chandra R (2010) Effect of bacteria treated and untreated post-methanated distillery effluent (PMDE) on seed germination, seedling growth and amylase activity in *Phaseolus mungo* L. *Hazard Mater* 180(1–3):730–734
- Cao Y, Hu Y, Sun J, Hou B (2010) Explore various co-substrates for simultaneous electricity generation and Congo red degradation in air-cathode single-chamber microbial fuel cell. *Bioelectrochemistry* 79(1):71–76
- Chang IS, Jang JK, Gil GC, Kim M, Kim HJ, Cho BW, Kim BH (2004) Continuous determination of biochemical oxygen demand using microbial fuel cell type biosensor. *Biosens Bioelectron* 19(6):607–613
- Chen BY (2002) Understanding decolorization characteristics of reactive azo dyes by *Pseudomonas luteola*: toxicity and kinetics. *Process Biochem* 38(3):437–446
- Chen WM, Laevens S, Lee TM, Coenye T, De Vos P, Mergeay M, Vandamme P (2001) *Ralstonia taiwanensis* sp. nov. isolated from root nodules of Mimosa species and sputum of a cystic fibrosis patient. *Int J Syst Evol Microbiol* 51:1729–1735
- Chen BY, Yen CY, Hsueh CC (2009a) Cost-effective biostimulation strategy for wastewater decolorization using immobilized-cell systems. *Bioresour Technol* 100(12):2975–2981
- Chen BY, Yen CY, Chen WM, Chang CT, Wang CT, Hu YC (2009b) Exploring threshold operation criteria of biostimulation for azo dye decolorization using immobilized cell systems. *Bioresour Technol* 100(23):5763–5770
- Chen BY, Chen WM, Kuo HY, Hsueh CC (2009c) Comparative assessment upon dye removal capability of indigenous bacterial strains from Lanyang Plain in northeast Taiwan. *J Hazard Mater* 161(1):526–533
- Chen BY, Zhang MM, Chang CT, Ding Y, Lin KL, Chiou CS, Hsueh CC, Xu H (2010a) Assessment upon azo dye decolorization and bioelectricity generation by *Proteus hauseri*. *Bioresour Technol* 101(12):4737–4741
- Chen BY, Wang YM, Ng IS, Zhang MM (2010b) Understanding interactive characteristics of bioelectricity generation and reductive decolorization using *Proteus hauseri*. *Bioresour Technol* (in press)
- Cheng S, Logan BE (2007) Ammonia treatment of carbon cloth anodes to enhance power generation of microbial fuel cells. *Electrochim Commun* 9(3):492–496
- Cheng S, Liu H, Logan BE (2006) Increased performance of single-chamber microbial fuel cells using an improved cathode structure. *Electrochim Commun* 8(3):489–494
- Du Z, Li H, Gu T (2007) A state of the art review on microbial fuel cells: a promising technology for wastewater treatment and bioenergy. *Biotechnol Adv* 25(5):464–482
- Erable B, Vandecandelaere I, Faimali M, Delia ML, Etcheverry L, Vandamme P, Bergel A (2010) Marine aerobic biofilm as biocathode catalyst. *Bioelectrochemistry* 78(1):51–56
- Fan Y, Hu H, Liu H (2007) Enhanced Coulombic efficiency and power density of air-cathode microbial fuel cells with an improved cell configuration. *J Power Sources* 171(2):348–354
- Fornero JJ, Rosenbaum M, Cotta MA, Angenent LT (2008) Microbial fuel cell performance with a pressurized cathode chamber. *Environ Sci Technol* 42(22):8578–8584
- Gil GC, Chang IS, Kim BH, Kim M, Jang JY, Park HS (2003) Operational parameters affecting the performance of a mediator-less microbial fuel cell. *Biosens Bioelectron* 18(4):327–334
- Gogate PR, Pandit AB (2004) A review of imperative technologies for wastewater treatment II: hybrid methods. *Adv Environ Res* 8(3–4):553–597
- Hsueh CC, Chen BY, Yen CY (2009) Understanding effects of chemical structure on azo dye decolorization characteristics by *Aeromonas hydrophila*. *J Hazard Mater* 167(1–3):995–1001
- Li Z, Zhang X, Lin J, Han S, Lei L (2010) Azo dye treatment with simultaneous electricity production in an anaerobic-aerobic sequential reactor and microbial fuel cell coupled system. *Bioresour Technol* 101(12):4440–4445

- Logan BE (2008) Microbial fuel cells. Wiley-Interscience Inc., New York, USA, p 18
- Logan BE, Hamelers B, Rozendal R, Schröder U, Keller J, Freguia S, Aelterman P, Verstraete W, Rabaey K (2006) Microbial fuel cells: methodology and technology. Environ Sci Technol 40(17):5181–5192
- Lorenzo MD, Scott K, Curtis TP, Head IM (2010) Effect of increasing anode surface area on the performance of a single chamber microbial fuel cell. Chem Eng J 156(1):40–48
- Maier J, Kandlbauer A, Erlacher A, Paulo AC, Gübitz GM (2004) A new alkali-thermostable azoreductase from *Bacillus* sp. Strain SF. Appl Environ Microbiol 70(2): 837–844
- Mohanakrishna G, Venkata Mohan S, Sarma PN (2010) Bioelectrochemical treatment of distillery wastewater in microbial fuel cell facilitating decolorization and desalination along with power generation. Hazard Mater 177(1–3):487–494
- Moon H, Chang IS, Kang KH, Jang JK, Kim BH (2004) Improving the dynamic response of a mediator-less microbial fuel cell as a biochemical oxygen demand (BOD) sensor. Biotechnol Lett 26:1717–1721
- Moon H, Chang IS, Kim BH (2006) Continuous electricity production from artificial wastewater using a mediator-less microbial fuel cell. Bioresour Technol 97(4):621–627
- Page RD (1996) TreeView: an application to display phylogenetic trees on personal computers. Comput Appl Biosci 12:357–358
- Pant D, Bogaert GV, Diels L, Vanbroekhoven K (2010) A review of the substrates used in microbial fuel cells (MFCs) for sustainable energy production. Bioresour Technol 101(6):1533–1543
- Park DH, Zeikus JG (2003) Improved fuel cell and electrode designs for producing electricity from microbial degradation. Biotechnol Bioeng 81(3):348–355
- Pham H, Jang JK, Chang IS, Kim BH (2004) Improvement of cathode reaction of a mediatorless microbial fuel cell. Microbiol Biotechnol 14(2):324–329
- Powers EM (1995) Efficacy of the Ryu nonstaining KOH technique for rapidly determining gram reactions of foodborne and waterborne bacteria and yeasts. Appl Environ Microbiol 61:3756–3758
- Rabaey K, Keller J (2008) Microbial fuel cell cathodes: from bottleneck to prime opportunity? Water Sci Technol 57:655–659
- Shih YH, Tso CP, Tung LY (2010) Rapid degradation of methyl orange with nanoscale zerovalent iron particles. Environ Eng Manage 20(3):137–143
- Shu HY, Chang MC, Fan HJ (2004) Decolorization of azo dye acid violet 1 by the V/H₂O₂ process and optimization of operating parameters. J Hazard Mater 113(1–3):201–208
- Sun J, Hu Y, Bi Z, Cao Y (2009a) Improved performance of air-cathode single-chamber microbial fuel cell for wastewater treatment using microfiltration membranes and multiple sludge inoculation. J Power Sources 187(2):471–479
- Sun J, Hu YY, Bi Z, Cao YQ (2009b) Simultaneous decolorization of azo dye and bioelectricity generation using a microfiltration membrane air-cathode single-chamber microbial fuel cell. Bioresour Technol 100(13):3185–3192
- Thompson JD, Gibson TJ, Plewniak F, Jeanmougin F, Higgins DG (1997) The CLUSTAL X windows interface. Flexible strategies for multiple sequence alignment aided by quality analysis tools. Nucleic Acids Res 25:4876–4882
- Virdis B, Rabaey K, Yuan Z, Keller J (2008) Microbial fuel cells for simultaneous carbon and nitrogen removal. Water Res 42(12):3013–3024
- Zhang MM, Chen WM, Chen BY, Chang CT, Hsueh CC, Ding YT, Lin KL, Xu HZ (2010) Comparative study on characteristics of azo dye decolorization by indigenous decolorizers. Bioresour Technol 101(8):2651–2656
- Zhao F, Harnisch F, Schröder U, Scholz F, Bogdano FP, Herrmann I (2005) Application of pyrolysed iron(II) phthalocyanine and CoTMPP based oxygen reduction catalysts as cathode materials in microbial fuel cells. Electrochim Commun 7(12):1405–1410